UROGENITAL IMAGING & CONTRAST MEDIA

Iran J Radiol. 2018 July; 15(3):e56003. doi: 10.5812/iranjradiol.56003.

Published online 2018 May 20. **Research Article**

In Vivo Tracking of Mesenchymal Stem Cell in Rat Genitalia with Erectile Dysfunction Labeled by Superparamagnetic Iron Oxide Using Magnetic Resonance Imaging and Its Therapeutic Effect

Kyung Taek Oh,[1] Ngoc Ha Hoang,[2] So-Young Park,[3] Eun Seong Lee,[4] Jang Hwan Kim,[5] and Young Taik Oh[6,*]

[1]College of Pharmacy, Chung-Ang University, Dongjak-Gu, Seoul, Republic of Korea
[2]Department of Pharmaceutics, Hanoi University of Pharmacy, Hanoi, Vietnam
[3]Laboratory of Pharmacognosy, College of Pharmacy, Dankook University, Dongnam-Gu, Cheonan, Republic of Korea
[4]Division of Biotechnology, The Catholic University of Korea, Wonmi-gu, Bucheon-si, Republic of Korea
[5]Department of Urology, College of Medicine, Yonsei University, Seoul, Republic of Korea
[6]Department of Radiology and Research Institute of Radiological Science, College of Medicine, Yonsei University, Seodaemun-gu, Seoul, Republic of Korea

[*]*Corresponding author*: Young Taik Oh, Department of Radiology and Research Institute of Radiological Science, College of Medicine, Yonsei University, 50 Yonsei-Ro, Seodaemun-gu, Seoul, 03722, Republic of Korea, E-mail: oytaik@yuhs.ac

Received 2017 June 23; **Revised** 2017 December 27; **Accepted** 2018 January 02.

Abstract

Background: Molecular imaging with nanoparticles makes non-invasive monitoring of target cells without sacrifice of subjects and repeated evaluation possible.
Objectives: To evaluate the imaging feasibility of a rat animal model with erectile dysfunction (ED) by bilateral cavernosal nerve injury using human mesenchymal stem cells (MSCs) labeled with superparamagnetic iron oxide (SPIO) and simultaneously to evaluate the beneficial effect of MSCs on ED.
Materials and Methods: Thirty-six rats were injected with MSCs labeled with SPIO particle into the corpus cavernosum after bilateral cavernosal nerve injury. In vivo MR imaging was serially performed up to 16 weeks using 1.5 T clinical scanner. After MR imaging, the penile specimens were evaluated for the expression of transforming growth factor-β1 (TGF-β1) by polymerase chain reaction.
Results: MR imaging showed a drop in signal intensity at the injection site in the stem cell-injected group. The size of hypointensity was decreased in MSC-injected group in a time-dependent manner; whereas, signal void was not detected at the injection site in the control group. In addition, polymeric chain reaction (PCR) analyses of penile tissues from both groups revealed that the mRNA expression of TGF-β1 was significantly decreased in MSC-injected groups after 4 weeks of injection compared to the control group.
Conclusion: MSCs' beneficial effects on ED was monitored with MR imaging, which might be a valuable tool for tracking and therapeutic monitoring in the future clinical study of stem cell therapy in ED.

Keywords: Molecular Imaging, Nanoparticles, Stem Cells, Erectile Dysfunction, Transforming Growth Factor

1. Background

Cell therapy is a relatively new approach for treatment of diseases by introducing new cells into a tissue. Mesenchymal stem cells (MSC), in particular, are considered as an agent for cell therapy. In order to succeed in cell therapy, a reliable in vivo imaging method in localizing transplanted cells makes systematic investigation of cell therapy possible (1-4). Previous researches with immunohistological staining were not usable to trace the migration of transplanted cells in vivo. Instead, molecular imaging including nuclear imaging, optical imaging, and magnetic resonance (MR) imaging (5-7) allows visualization of targeted cells in living organisms. In particular, molecular imaging with nanoparticles makes non-invasive monitoring of target cells without sacrifice of subjects and repeated evaluation possible (8-11). Labeling cells with superparamagnetic iron oxide (SPIO) nanoparticles or a paramagnetic contrast agent gadolinium (12) or manganese (4, 13, 14) provides the possibility of detecting single cells or clusters of labeled cells within target tissues after either direct implantation or intravenous injection (15-17).

Prostate cancer is the second most frequent cancer in men in USA and it has the most rapidly increasing incidence in Korea. Prostate specific antigen (PSA) for screening of prostate cancer and trans-rectal ultrasound (TRUS)-guided biopsy allow the diagnosis of prostate cancer at

an early stage (4). Regardless, radical prostatectomy (RP) is a very common method in the treatment of prostate cancer (18). The major complication of RP is the erectile dysfunction (ED) (19), which is caused by loss of corporal smooth muscle cells and subsequent fibrosis of the corpus cavernosum by either direct damage or neuropraxia of the cavernous nerve, alone or with hemodynamic alterations. Nerve sparing surgery has been proposed to spare the erectile function (20). However, no satisfying results have been shown (21). Conversely, it has been reported that stem cell injection improves erectile function in the rat model with erection dysfunction (22).

2. Objectives

In this study, the rat animal model with ED by bilateral cavernosal nerve (CN) injury was established to evaluate the feasibility for imaging of MSC treatment. Therefore, MSCs isolated from human bone marrow were labeled with ferumoxides and were injected into the corpus cavernosum of rats. The serial in vivo tracking of labeled MSCs was performed by magnetic resonance (MR) imaging. The mRNA expression of transforming growth factor-β1 (TGF-β1) in rats injected with MSCs was compared to the control rats in order to evaluate the beneficial effect of MSCs on ED.

3. Materials and Methods

3.1. Animals and Cell Preparation

Animal protocols were approved by the animal studies committee at the medical research center of Yonsei University. Male Sprague-Dawley rats (SLC, Tokyo, Japan), weighing 140 $\pm$ 5 g, were housed under standard laboratory conditions (temperature 24 $\pm$ 2°C; humidity 50 $\pm$ 10%, 12-h day/night cycles). Prior to experiments, animals were allowed to acclimatize to the facility for one week, and were provided a standard chow diet and drinking water ab libitum. Animals were five weeks old on the first day of the exposure study.

Mesenchymal stem cells (MSCs) used in this study were donated by the department of orthopedic surgery in Yonsei University (Soeul, Korea). The MSCs were isolated from human bone marrow without hematological and bone marrow abnormality and were expanded in Dulbecco's Modified Eagle Medium (DMEM, Gibco, Carlsbad, CA, USA) + 10% fetal bovine serum (FBS, Gibco, Carlsbad, CA, USA) + penicillin-streptomycin (Invitrogen, Carlsbad, CA, USA) in a 37°C, 5% CO_2 incubator.

3.2. Labeling MSCs with SPIO

In order to label MSCs, we employed ferumoxides (Feridex IV, Bayer-Schering Pharma, Wayne, NJ, USA) as superparamagnetic iron oxide (SPIO) nanoparticles for intracellular magnetic labeling of stem cells to monitor cell trafficking by MR imaging, and protamine sulfate (American Pharmaceuticals Partner, Schaumburg, IL, USA) as a transfection agent (23, 24). Briefly, ferumoxides (50 μg/mL) and protamine sulfate (9 μg/mL) were added to the standard culture medium and mixed for 10 minutes with intermittent hand shakings, after which cells were incubated another 2 hours. The equal volume of the culture medium was then added to the cells, and cells were incubated in 37°C. After overnight incubation, the cells were washed twice with heparin containing phosphate buffered saline, collected, and counted for injection.

The efficiency of intracellular labeling of MSCs with SPIO was determined with Prussian blue staining. The labeled 1×10^6 cells were fixed with 95% alcohol and stained with 10% potassium ferrocyanide (Perl's reagent for Prussian blue staining) and 3.7% hydrochloric acid for 20 minutes, after which the cells were counterstained with nuclear fast red. Cells containing intra-cytoplasmic blue inclusions were considered as Prussian blue positive. The number of Prussian blue-stained and unstained cells were counted using hemocytometer ($\times$ 100) under an inverted microscope and labeling efficiency was determined by percentage of Prussian blue-stained positive cells over total cells.

3.3. Cavernosal Nerve Injury and MSC Injection

Thirty-six (five weeks old, 12 per group) rats were divided into 4 week, 8 week, and 16 week groups. Each group was further divided into two subgroups, control and stem cell groups (6 per subgroup). After anesthesia with an intraperitoneal injection of ketamine and xylazine, skin incision was made. After transection of bilateral cavernosal nerves, 1×10^6 MSCs in 0.02 mL media or 0.02 mL of cell-free media were injected into the corpus cavernosum of rats in stem cell groups or in control groups, respectively. After the injection, the penile base was strangulated for 30 seconds and then released.

3.4. In vivo MR imaging

MRI was obtained with a 1.5 T clinical MRI scanner with a micro-47 surface coil (InteraAchieva, Philips Medical Systems, Best, Netherlands). For in vivo penile MRI, the rats were anesthetized with an intraperitoneal injection of ketamine and xylazine and ferumoxides-labeled MSCs were visualized by gradient echo sequence with the following parameters: T1-turbo field echo sequence, shortest repetition time (TR) and echo time (TE), flip angle = 15°, matrix

= 256 × 256, number of averages = 6, field of view = 80 mm. Gradient echo MR imaging was very sensitive to detect the SPIO particles, which were detected as dark signal-intensity. If there was a spot with dark signal-intensity on injection site, we regarded that there were the SPIO-labeled MSCs.

3.5. Fibrosis Analysis with Reverse Transcriptase Polymerase Chain Reaction (RT-PCR)

For the fibrosis analysis, the rats were sacrificed at 4, 8, and 16 weeks of injection after MR imaging, and the penile tissues were collected. The expression of endogenous transforming growth factor (TGF)-β1 mRNA in the penis was evaluated by reverse transcriptase polymerase chain reaction (RT-PCR). Total RNA was isolated using TRIzol (Invitrogen, NY, USA) and then processed for the first-strand complementary DNA (cDNA) synthesis using reverse transcriptase with oligo (dT) primers (Invitrogen, NY, USA). The cDNA products were then amplified by PCR using T100TM Thermal Cycler (bio-Rad, Hercules, CA). Primer sequences were as follows; TGF-β1 forward 5'-GAT GAG ATC GAG TAC ATC TT-3', reverse 5'-CAC CGC CTC GGC TTG TCA CAT-3'; β-actin forward 5'-TCT ACA ATG AGC TGC GTG TG -3', reverse 5'-AAT GTC ACG CAC GAT TTC CC- 3'. The amplified PCR products were identified by electrophoresis using 1% agarose gels containing ethidium bromide and then visualized under UV light. The relative amount of TGF-β1 mRNA was calculated as its ratio to β-actin from the same template. The data are expressed as mean ± standard deviation (SD). Two group comparisons at the same period were evaluated by a one-way analysis of variance (ANOVA). Differences were considered statistically significant at $P < 0.05$. In addition, a two-way ANOVA analysis was performed between time and treatment. The statistical analysis was performed using IBM SPSS Statistics for Windows, Version 23.0. (Armonk, NY: IBM Corp.).

3.6. Histological Analysis

The penile tissues were retrieved and fixed in 4% paraformaldehyde. The specimens at the injection sites were cut at a thickness of 4 μm in the short-axis plane and stained with hematoxylin and eosin (H&E). Prussian blue staining was also performed to detect ferumoxides-labeled MSCs. The histological evaluation was performed under an inverted microscope.

4. Results

4.1. Intracellular Labeling of MSCs with SPIO

MSCs isolated from human bone marrow were labeled with ferumoxides as superparamagnetic iron oxide (SPIO) nanoparticles for intracellular magnetic labeling to monitor cell trafficking by MR imaging. The labeling efficacy was examined under a microscope after Prussian complex staining, which is a common stain to detect the presence of iron. As shown in Figure 1, the most MSCs were labelled with SPIO. The blue inclusions were easily detected at the intra-cytoplasmic areas, whereas extracellular blue inclusions were rarely examined.

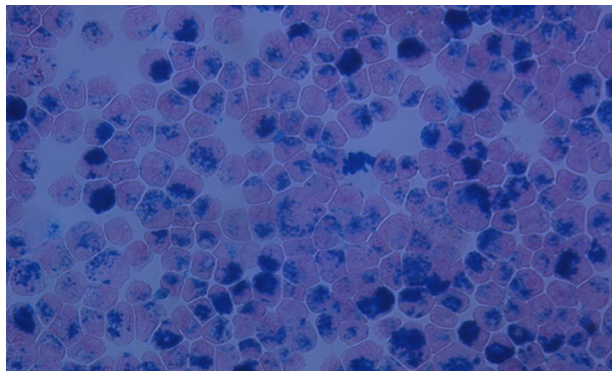

Figure 1. Prussian blue-stained Feridex-labeled mesenchymal stem cells. Mesenchymal stem cells were labeled with superparamagnetic iron oxide (SPIO) nanoparticles for intracellular magnetic labeling and the efficacy of the labeling was examined under a microscope after Prussian blue staining (× 1000).

4.2. In vivo MR Tracking of MSCs

SPIO labeled MSCs were then injected into the corpus cavernosum of rats after radical prostatectomy. During the experiments, one rat of MSC-injected group died in four weeks, and the other one died in 8 weeks. The rest of the 34 rats was examined with MRI for in vivo tracking of MSCs (Figure 2). After 4 weeks of injection into the corpus cavernosum of the rats, the presence of SPIO-labeled MSCs appeared as a hypointensity at the injection site demonstrated by T1-weighted gradient-echo MR imaging (Figure 2A). Follow-up serial MR imaging revealed the decreased sizes of hypointensity. After 12 weeks, most hypointensities were difficult to define (Figure 2C). However, the hypointensity was not observed at the injection site in the control group injected with cell-free media (Figure 2E).

4.3. Histological Analysis

In order to confirm the presence of SPIO-labeled MSCs at the injection sites, the tissues collected from rats at 8 weeks of injection were stained with Prussian blue and examined under a microscope. The intense intracellular blue staining was observed with Prussian blue staining, indicating intracellular iron-labeled cells, with iron exclusions from the nucleus. The area of blue staining was cor-

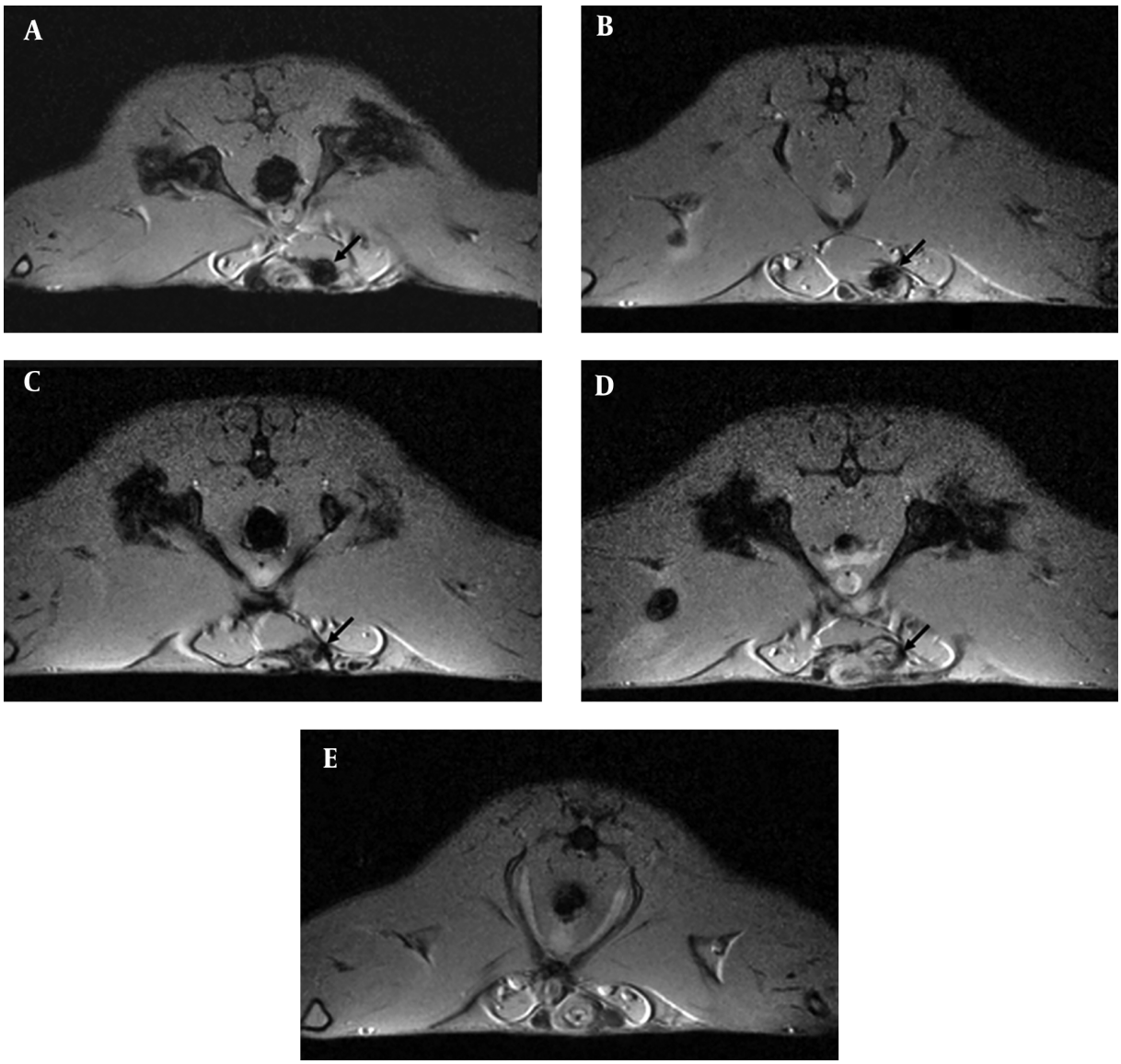

Figure 2. In vivo magnetic resonance (MR) imaging with superparamagnetic iron oxide (SPIO)-labeled mesenchymal stem cells after transection of bilateral cavernosal nerves. A - E, Short axis T1-weighted gradient-echo MR imaging of rats showed the distinct hypointensity (indicated by arrows) at the penis 4 weeks (A) after injection. The size of hypointensity became smaller gradually in rats after 8 (B), 12 (C), and 16 (D) weeks of injection. Conversely, no signal change was detected in a media-injected control rat (E).

responding to the hypointensity examined by MR imaging (Figure 3).

4.4. RT-PCR Analysis for the mRNA Expression of TGF-β1

The expression of TGF-β1 was investigated from the penile tissues of rats by semi-quantitative reverse transcription-polymerase chain reaction (RT-PCR). The band intensity was expressed as the ratio of TGF-β1 to β-actin (Table 1). As shown in Figure 4, rats injected with cell-free media after RP showed a significant increase of TGF-β1 mRNA expression compared to untreated control rats. Furthermore, the penile tissues from rats treated with the stem cells for 4 weeks after RP showed a significant decrease of TGF-β1 compared to rats in cell-free media injected control groups. However, the expressions of TGF-β1 in rats treated with the stem cells for 8 or 16 weeks were not significantly different from rats in media-injected control groups (Figure 4A and 4B).

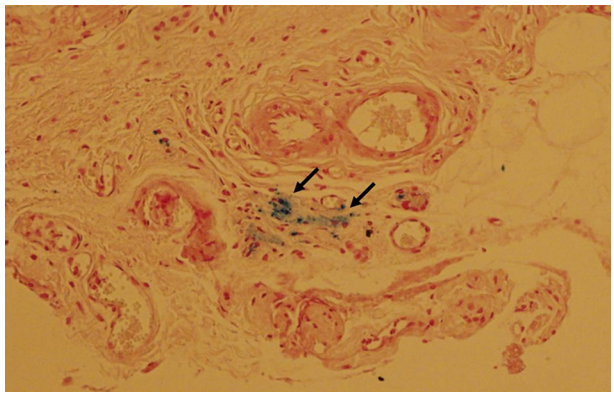

Figure 3. Histological analysis of superparamagnetic iron oxide (SPIO)-labeled mesenchymal stem cells with Prussian blue staining. Rats at 8 weeks after injection of SPIO-labeled mesenchymal stem cells into the corpus cavernosum were sacrificed and the tissue was stained with Prussia blue staining. Hypointensities detected by MR imaging were visible as blue stained area (indicated by arrows) by histological examination with Prussian blue staining, indicating the presence of the intracytoplasmic SPIO particles in the hypointensity.

Table 1. RT-PCR Analysis of TGF-β1 mRNA Expression[a]

	4 w	8 w	16 w
Control groups	0.617	0.432	0.512
	0.614	0.456	0.39
	0.566	0.352	0.408
	0.591	0.347	0.359
	0.535	0.309	0.316
	0.55	0.366	0.266
Ave. ± Std. Dev.	0.579 ± 0.0339	0.377 ± 0.0557	0.375 ± 0.0845
MSC injected groups	0.556	0.487	0.636
	0.521	0.539	0.522
	0.471	0.487	0.575
	0.542	0.373	0.504
	0.397	0.334	0.329
	0.484	0.35	0.275
Ave. ± Std. Dev.	0.495 ± 0.0582	0.428 ± 0.0863	0.474 ± 0.0142

Abbreviations: MSC, mesenchymal stem cell; RT-PCR, reverse transcription-polymerase chain reaction; TGF-β1, transforming growth factor-β1; W, week.
[a]All data indicated the ratio of TGF- β1 and β-actin (TGF- β1 / β-actin) and Ave. and Std. Dev. indicated the average value and standard deviation, respectively.

5. Discussion

Cell therapy is the process of introducing new cells into a tissue for the treatment of a disease, and various cell types are used in experimental models. In particular, MSCs are considered as an agent for cell therapy due to their plasticity, established isolation procedures and capacity for ex vivo expansion (25). In order to achieve success in cell therapy, noninvasive in vivo imaging methods are required for monitoring the temporal-spatial migration of transplanted cells into a targeted organ. Much research has been performed to find good techniques to determine the localization of therapeutic cells transplanted into the organs. Clinical nuclear medicine approaches exhibited relatively short monitoring period of 2 - 3 days following the transplantation and possible damage to DNA (26). In addition, optical and bioluminescent imaging approaches were limited in preclinical experiments due to the introduction of toxic agents such as Qdots (27). Conversely, MR imaging with SPIO nanoparticles has several advantages such as high spatial resolution, long-term monitoring, and no-toxicity due to the biodegradable and metabolizable nanoparticles (28). Therefore, in this study, the MR imaging was employed to track the labeling MSCs with ferumoxides, FDA-approved labeling agent for long-term monitoring of transplanted cell-therapy into the clinic (29-32).

ED limits the quality of life of man and his partner. ED is known to be caused by the damage of penile cavernous smooth muscle cells and sinus endothelial cells by various metabolic conditions or mechanical manipulations (33, 34). In addition, RP, a dominant therapy for clinically localized prostate cancer, is one of the main causes of ED due to the injury of CN (35, 36). It is reported that many patients following RP lost erectile ability coupled with a gradual reduction in the size of the penis, increased apoptosis in penile tissues of rats after denervation, and decreased penile size. Several in vitro and in vivo studies reported the possible treatment of ED such as oral phosphodiesterase type 5 (PDE5) inhibitors and mesenchymal stem cell-based cell and gene therapies. Unfortunately, PDE5 inhibitors are not effective for the patients with diabetes, non-nerve sparing radical prostatectomy, and high disease severity (37, 38). It was recently reported that transplanted human MSCs have the potential to differentiate toward sinus endothelial cells or penile cavernous smooth muscle cells, which are critical to maintain and regulate ED (39, 40). In this study, MSCs was injected into the corpus cavernosum of a rat with RP without nerve sparing and a clinical MR scanner was applied to identify transplanted MSCs labeled with SPIO particles in in vivo rat models after radical prostatectomy. Intracavernosal MSCs injection sites in the rat penis appeared as hypointensity on in vivo MR imaging. The SPIO nanoparticles shorten the T1, T2 and T2* relaxation times of water or tissue and have a high T2 relaxivity/T1 relaxivity ratio and significant capacity to reduce MRI signal, which can be emphasized by using spin echo sequences with longer echo time and by using gradient echo sequences (41). Therefore, intracellular SPIO of transplanted cells could be readily detected as a hypointensity

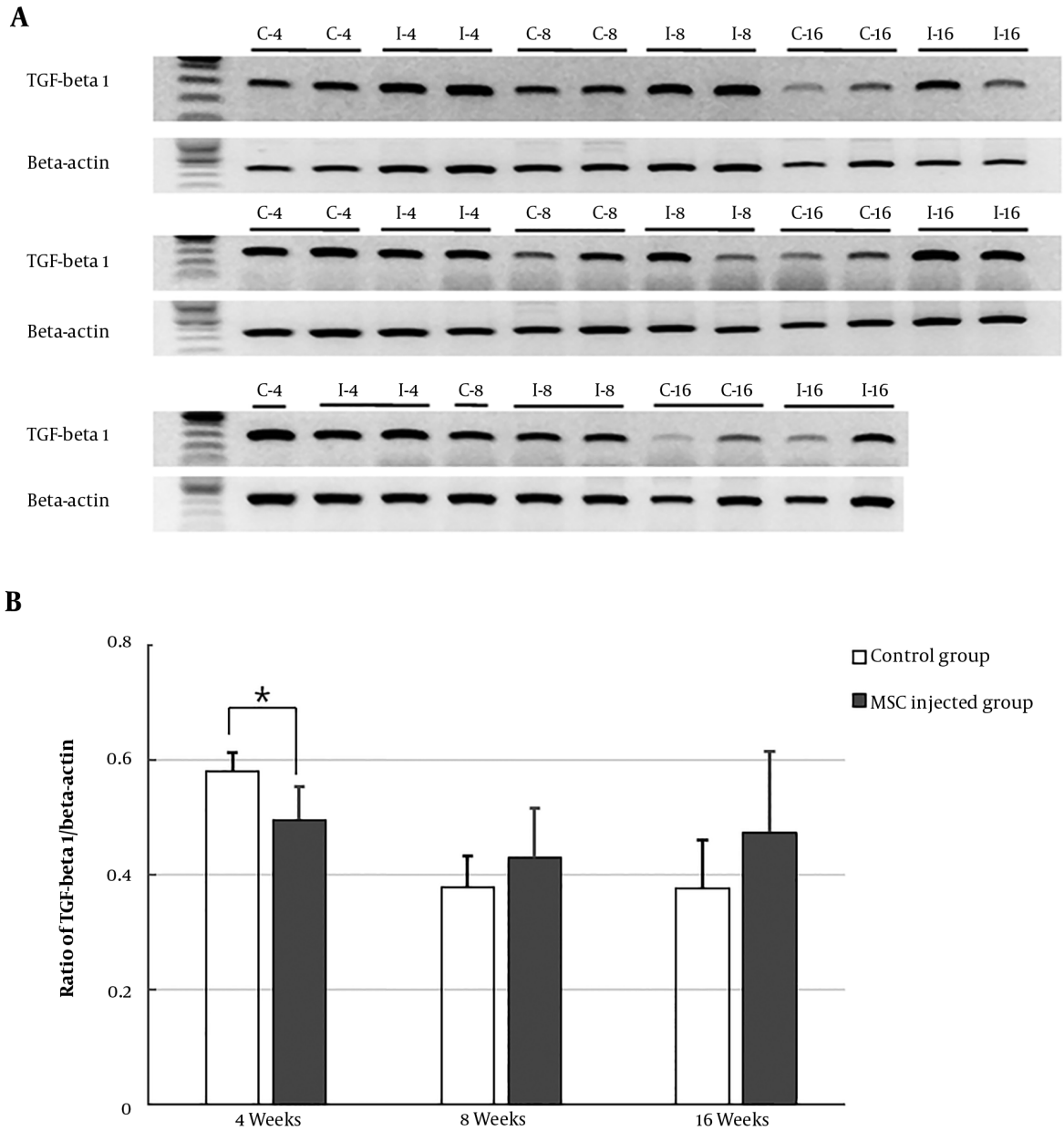

Figure 4. Reverse transcription-polymerase chain reaction (RT-PCR) analysis of transforming growth factor- β1 (TGF-β1) mRNA expression. A, Penile tissues from rats treated with the stem cells for 4, 8, or 16 weeks were collected and the expression of TGF-β1 was analyzed by RT-PCR. (I; stem cell injected groups and C; control groups). B, Graphs showing changes in the ratio of TGF-β1/ β-actin in the tissues. All data represent means $\pm$ standard error from six rats from each group as a function of time. *, $P < 0.01$, different from the control group in one-way ANOVA analysis. A two-way ANOVA between time and treatment indicated $P < 0.05$.

(dark lesion) by MR imaging. On the other hand, the hypointensity showed the decrease in size along the serial MR images. They were hardly detected after 12 weeks due to death, migration, and differentiation of MSCs into the smooth muscles and endothelial cells (42). However, the exact mechanisms of disappearance of a hypointensity require further investigation.

TGF-β1 is one of the cytokines with a chemotactic role in inflammatory cells and fibroblasts (43). It can modulate extracellular matrix by increasing the synthesis of its

components and inhibiting the expression of hydrolytic proteinases (44). Hypoxia can induce TGF-β1, which increases collagen synthesis in human corpus cavernosal smooth muscle cells in culture (45). Conversely, hypoxia inhibits the production of prostaglandin E1 (PGE1), which suppresses collagen synthesis and fibrosis induced by TGF-β1 in human corpus cavernosal smooth muscle (46). A high protein and mRNA expression of TGF-β1 in neurotomy group suggests that ischemia and hypoxia may have occurred in the penile tissues of rats after denervation (46). It was also reported that the levels of TGF-β1 in plasma were significantly increased in patients with ED, especially those with a vasculogenic cause. It implicated that the increase in TGF-β1 induces cavernosal fibrosis and ED after RD (47). Therefore, increased expression of TGF-β1 in penile tissue may be one of the important factors for the ED caused by bilateral CN ablation. In the present study, we ablated both CNs in a rat model, which mimics patients after RP with no nerve sparing. The neurotomized rats in the 4-weeks group showed the significant increase of mRNA expression of TGF-β1 compared to the normal rats. These results are in agreement with the previous report saying that the expression of TGF-β1 in neurotomized group was much higher than in the sham-operated group both at the mRNA and protein level (48). Furthermore, treatment of MSCs in neurotomized rats exhibited a significant decrease of TGF-β1 compared to the rats in the neurotomized group and implied reduction of hypoxia or ischemia induced by neurotomy. These results suggested the potential beneficial effects of MSC injection to treat ED after radical prostatectomy.

In summary, clinical MR imaging was applied to identify transplanted MSCs labeled with SPIO particle in in vivo rat model after RP. The results demonstrated that MSCs labeled with SPIO could be tracked in vivo in the rat genitalia of RP model up to 12 weeks. In addition, rats injected with MSCs showed significantly lower levels of TGF-β1 compared to the control rats, suggesting MSCs' beneficial effects on ED induced by RP. In conclusion, these results suggest that MR imaging might be a viable tool for tracking and therapeutic monitoring in the future clinical study of stem cell therapy in ED.

Footnotes

Conflict of Interests: The authors declare that there is no conflict of interest.

Funding/Support: This work was supported by the national research foundation of Korea (NRF) grant funded by the Korea government (MSIP) (NRF-2014R1A2A1A11050094).

References

1. Kircher MF, Gambhir SS, Grimm J. Noninvasive cell-tracking methods. *Nat Rev Clin Oncol*. 2011;**8**(11):677–88. doi: 10.1038/nrclinonc.2011.141. [PubMed: 21946842].
2. Reagan MR, Kaplan DL. Concise review: Mesenchymal stem cell tumor-homing: detection methods in disease model systems. *Stem Cells*. 2011;**29**(6):920–7. doi: 10.1002/stem.645. [PubMed: 21557390]. [PubMed Central: PMC4581846].
3. Nam SY, Ricles LM, Suggs LJ, Emelianov SY. In vivo ultrasound and photoacoustic monitoring of mesenchymal stem cells labeled with gold nanotracers. *PLoS One*. 2012;**7**(5). e37267. doi: 10.1371/journal.pone.0037267. [PubMed: 22615959]. [PubMed Central: PMC3353925].
4. Tornblom M, Eriksson H, Franzen S, Gustafsson O, Lilja H, Norming U, et al. Lead time associated with screening for prostate cancer. *Int J Cancer*. 2004;**108**(1):122–9. doi: 10.1002/ijc.11554. [PubMed: 14618626].
5. Terreno E, Castelli DD, Viale A, Aime S. Challenges for molecular magnetic resonance imaging. *Chem Rev*. 2010;**110**(5):3019–42. doi: 10.1021/cr100025t. [PubMed: 20415475].
6. Pysz MA, Gambhir SS, Willmann JK. Molecular imaging: current status and emerging strategies. *Clin Radiol*. 2010;**65**(7):500–16. doi: 10.1016/j.crad.2010.03.011. [PubMed: 20541650]. [PubMed Central: PMC3150531].
7. Signore A, Mather SJ, Piaggio G, Malviya G, Dierckx RA. Molecular imaging of inflammation/infection: nuclear medicine and optical imaging agents and methods. *Chem Rev*. 2010;**110**(5):3112–45. doi: 10.1021/cr900351r. [PubMed: 20415479].
8. Kircher MF, de la Zerda A, Jokerst JV, Zavaleta CL, Kempen PJ, Mittra E, et al. A brain tumor molecular imaging strategy using a new triple-modality MRI-photoacoustic-Raman nanoparticle. *Nat Med*. 2012;**18**(5):829–34. doi: 10.1038/nm.2721. [PubMed: 22504484]. [PubMed Central: PMC3422133].
9. Tassa C, Shaw SY, Weissleder R. Dextran-coated iron oxide nanoparticles: a versatile platform for targeted molecular imaging, molecular diagnostics, and therapy. *Acc Chem Res*. 2011;**44**(10):842–52. doi: 10.1021/ar200084x. [PubMed: 21661727]. [PubMed Central: PMC3182289].
10. Jokerst JV, Gambhir SS. Molecular imaging with theranostic nanoparticles. *Acc Chem Res*. 2011;**44**(10):1050–60. doi: 10.1021/ar200106e. [PubMed: 21919457]. [PubMed Central: PMC3196845].
11. Cho EC, Glaus C, Chen J, Welch MJ, Xia Y. Inorganic nanoparticle-based contrast agents for molecular imaging. *Trends Mol Med*. 2010;**16**(12):561–73. doi: 10.1016/j.molmed.2010.09.004. [PubMed: 21074494]. [PubMed Central: PMC3052982].
12. Arifin DR, Long CM, Gilad AA, Alric C, Roux S, Tillement O, et al. Trimodal gadolinium-gold microcapsules containing pancreatic islet cells restore normoglycemia in diabetic mice and can be tracked by using US, CT, and positive-contrast MR imaging. *Radiology*. 2011;**260**(3):790–8. doi: 10.1148/radiol.11101608. [PubMed: 21734156]. [PubMed Central: PMC3157003].
13. Kim T, Momin E, Choi J, Yuan K, Zaidi H, Kim J, et al. Mesoporous silica-coated hollow manganese oxide nanoparticles as positive T1 contrast agents for labeling and MRI tracking of adipose-derived mesenchymal stem cells. *J Am Chem Soc*. 2011;**133**(9):2955–61. doi: 10.1021/ja1084095. [PubMed: 21314118]. [PubMed Central: PMC3048840].
14. Yang J, Lim EK, Lee ES, Suh JS, Haam S, Huh YM. Magnetoplex based on MnFe2O4 nanocrystals for magnetic labeling and MR imaging of human mesenchymal stem cells. *J Nanoparticle Res*. 2010;**12**(4):1275–83. doi: 10.1007/s11051-009-9837-1.
15. Cromer Berman SM, Walczak P, Bulte JW. Tracking stem cells using magnetic nanoparticles. *Wiley Interdiscip Rev Nanomed Nanobiotechnol*. 2011;**3**(4):343–55. doi: 10.1002/wnan.140. [PubMed: 21472999]. [PubMed Central: PMC3193153].

16. Ahrens ET, Bulte JW. Tracking immune cells in vivo using magnetic resonance imaging. *Nat Rev Immunol*. 2013;**13**(10):755–63. doi: 10.1038/nri3531. [PubMed: 24013185]. [PubMed Central: PMC3886235].
17. Liu G, Wang Z, Lu J, Xia C, Gao F, Gong Q, et al. Low molecular weight alkyl-polycation wrapped magnetite nanoparticle clusters as MRI probes for stem cell labeling and in vivo imaging. *Biomaterials*. 2011;**32**(2):528–37. doi: 10.1016/j.biomaterials.2010.08.099. [PubMed: 20869767].
18. Engel J, Bastian PJ, Baur H, Beer V, Chaussy C, Gschwend JE, et al. Survival benefit of radical prostatectomy in lymph node-positive patients with prostate cancer. *Eur Urol*. 2010;**57**(5):754–61. doi: 10.1016/j.eururo.2009.12.034. [PubMed: 20106588].
19. Ward JF, Slezak JM, Blute ML, Bergstralh EJ, Zincke H. Radical prostatectomy for clinically advanced (cT3) prostate cancer since the advent of prostate-specific antigen testing: 15-year outcome. *BJU Int*. 2005;**95**(6):751–6. doi: 10.1111/j.1464-410X.2005.05394.x. [PubMed: 15794776].
20. Walsh PC, Lepor H, Eggleston JC. Radical prostatectomy with preservation of sexual function: anatomical and pathological considerations. *Prostate*. 1983;**4**(5):473–85. [PubMed: 6889192].
21. Quinlan DM, Epstein JI, Carter BS, Walsh PC. Sexual function following radical prostatectomy: influence of preservation of neurovascular bundles. *J Urol*. 1991;**145**(5):998–1002. [PubMed: 2016818].
22. Bochinski D, Lin GT, Nunes L, Carrion R, Rahman N, Lin CS, et al. The effect of neural embryonic stem cell therapy in a rat model of cavernosal nerve injury. *BJU Int*. 2004;**94**(6):904–9. doi: 10.1111/j.1464-410X.2003.05057.x. [PubMed: 15476533].
23. Arbab AS, Yocum GT, Kalish H, Jordan EK, Anderson SA, Khakoo AY, et al. Efficient magnetic cell labeling with protamine sulfate complexed to ferumoxides for cellular MRI. *Blood*. 2004;**104**(4):1217–23. doi: 10.1182/blood-2004-02-0655. [PubMed: 15100158].
24. Arbab AS, Yocum GT, Wilson LB, Parwana A, Jordan EK, Kalish H, et al. Comparison of transfection agents in forming complexes with ferumoxides, cell labeling efficiency, and cellular viability. *Mol Imaging*. 2004;**3**(1):24–32. doi: 10.1162/153535004773861697. [PubMed: 15142409].
25. Caplan AI. Review: mesenchymal stem cells: cell-based reconstructive therapy in orthopedics. *Tissue Eng*. 2005;**11**(7-8):1198–211. doi: 10.1089/ten.2005.11.1198. [PubMed: 16144456].
26. Sheikh AY, Wu JC. Molecular imaging of cardiac stem cell transplantation. *Curr Cardiol Rep*. 2006;**8**(2):147–54. [PubMed: 16524542].
27. Zhang T, Stilwell JL, Gerion D, Ding L, Elboudwarej O, Cooke PA, et al. Cellular effect of high doses of silica-coated quantum dot profiled with high throughput gene expression analysis and high content cellomics measurements. *Nano Lett*. 2006;**6**(4):800–8. doi: 10.1021/nl0603350. [PubMed: 16608287]. [PubMed Central: PMC2730586].
28. Sun C, Lee JS, Zhang M. Magnetic nanoparticles in MR imaging and drug delivery. *Adv Drug Deliv Rev*. 2008;**60**(11):1252–65. doi: 10.1016/j.addr.2008.03.018. [PubMed: 18558452]. [PubMed Central: PMC2702670].
29. Arbab AS, Bashaw LA, Miller BR, Jordan EK, Bulte JW, Frank JA. Intracytoplasmic tagging of cells with ferumoxides and transfection agent for cellular magnetic resonance imaging after cell transplantation: methods and techniques. *Transplantation*. 2003;**76**(7):1123–30. doi: 10.1097/01.TP.0000089237.39220.83. [PubMed: 14557764].
30. Andreas K, Georgieva R, Ladwig M, Mueller S, Notter M, Sittinger M, et al. Highly efficient magnetic stem cell labeling with citrate-coated superparamagnetic iron oxide nanoparticles for MRI tracking. *Biomaterials*. 2012;**33**(18):4515–25. doi: 10.1016/j.biomaterials.2012.02.064. [PubMed: 22445482].
31. Frank JA, Miller BR, Arbab AS, Zywicke HA, Jordan EK, Lewis BK, et al. Clinically applicable labeling of mammalian and stem cells by combining superparamagnetic iron oxides and transfection agents. *Radiology*. 2003;**228**(2):480–7. doi: 10.1148/radiol.2281020638. [PubMed: 12819345].
32. Arbab AS, Liu W, Frank JA. Cellular magnetic resonance imaging: current status and future prospects. *Expert Rev Med Devices*. 2006;**3**(4):427–39. doi: 10.1586/17434440.3.4.427. [PubMed: 16866640].
33. Miralles-Garcia JM, Garcia-Diez LC. Specific aspects of erectile dysfunction in endocrinology. *Int J Impot Res*. 2004;**16 Suppl 2**:S10–2. doi: 10.1038/sj.ijir.3901237. [PubMed: 15496851].
34. Sainz I, Amaya J, Garcia M. Erectile dysfunction in heart disease patients. *Int J Impot Res*. 2004;**16 Suppl 2**:S13–7. doi: 10.1038/sj.ijir.3901238. [PubMed: 15496852].
35. Iacono F, Giannella R, Somma P, Manno G, Fusco F, Mirone V. Histological alterations in cavernous tissue after radical prostatectomy. *J Urol*. 2005;**173**(5):1673–6. doi: 10.1097/01.ju.0000154356.76027.4f. [PubMed: 15821546].
36. Walsh PC, Donker PJ. Impotence following radical prostatectomy: insight into etiology and prevention. 1982. *J Urol*. 2002;**167**(2 Pt 2):1005–10. [PubMed: 11905870].
37. Carson CC, Lue TF. Phosphodiesterase type 5 inhibitors for erectile dysfunction. *BJU Int*. 2005;**96**(3):257–80. doi: 10.1111/j.1464-410X.2005.05614.x. [PubMed: 16042713].
38. Manecke RG, Mulhall JP. Medical treatment of erectile dysfunction. *Ann Med*. 1999;**31**(6):388–98. [PubMed: 10680853].
39. Song YS, Lee HJ, Park IH, Kim WK, Ku JH, Kim SU. Potential differentiation of human mesenchymal stem cell transplanted in rat corpus cavernosum toward endothelial or smooth muscle cells. *Int J Impot Res*. 2007;**19**(4):378–85. doi: 10.1038/sj.ijir.3901539. [PubMed: 17460699].
40. Song H, Chang W, Lim S, Seo HS, Shim CY, Park S, et al. Tissue transglutaminase is essential for integrin-mediated survival of bone marrow-derived mesenchymal stem cells. *Stem Cells*. 2007;**25**(6):1431–8. doi: 10.1634/stemcells.2006-0467. [PubMed: 17347495].
41. Wang YX, Hussain SM, Krestin GP. Superparamagnetic iron oxide contrast agents: physicochemical characteristics and applications in MR imaging. *Eur Radiol*. 2001;**11**(11):2319–31. doi: 10.1007/s003300100908. [PubMed: 11702180].
42. Bivalacqua TJ, Deng W, Kendirci M, Usta MF, Robinson C, Taylor BK, et al. Mesenchymal stem cells alone or ex vivo gene modified with endothelial nitric oxide synthase reverse age-associated erectile dysfunction. *Am J Physiol Heart Circ Physiol*. 2007;**292**(3):H1278–90. doi: 10.1152/ajpheart.00685.2006. [PubMed: 17071732].
43. Postlethwaite AE, Keski-Oja J, Moses HL, Kang AH. Stimulation of the chemotactic migration of human fibroblasts by transforming growth factor beta. *J Exp Med*. 1987;**165**(1):251–6. [PubMed: 3491869]. [PubMed Central: PMC2188256].
44. Laping NJ, Grygielko E, Mathur A, Butter S, Bomberger J, Tweed C, et al. Inhibition of transforming growth factor (TGF)-beta1-induced extracellular matrix with a novel inhibitor of the TGF-beta type I receptor kinase activity: SB-431542. *Mol Pharmacol*. 2002;**62**(1):58–64. [PubMed: 12065755].
45. Moreland RB, Traish A, McMillin MA, Smith B, Goldstein I, Saenz de Tejada I. PGE1 suppresses the induction of collagen synthesis by transforming growth factor-beta 1 in human corpus cavernosum smooth muscle. *J Urol*. 1995;**153**(3 Pt 1):826–34. [PubMed: 7861547].
46. Moreland RB. Is there a role of hypoxemia in penile fibrosis: a viewpoint presented to the Society for the Study of Impotence. *Int J Impot Res*. 1998;**10**(2):113–20. [PubMed: 9647948].
47. Ryu JK, Song SU, Choi HK, Seong DH, Yoon SM, Kim SJ, et al. Plasma transforming growth factor-beta1 levels in patients with erectile dysfunction. *Asian J Androl*. 2004;**6**(4):349–53. [PubMed: 15546028].
48. Leungwattanakij S, Bivalacqua TJ, Usta MF, Yang DY, Hyun JS, Champion HC, et al. Cavernous neurotomy causes hypoxia and fibrosis in rat corpus cavernosum. *J Androl*. 2003;**24**(2):239–45. [PubMed: 12634311].